

Gd impurity effect on the magnetic and electronic properties of hexagonal Sr ferrites: A case study by DFT

Masomeh Taghipour, Mohammad Yousefi, Reza Fazaeli, Masoud Darvishganji

Citation: Chin. Phys. B . 2020, 29(7): 077505 . **doi:** 10.1088/1674-1056/ab8d9f
Journal homepage: http://cpb.iphy.ac.cn; http://iopscience.iop.org/cpb

What follows is a list of articles you may be interested in

Degenerate antiferromagnetic states in spinel oxide LiV_2O_4

Ben-Chao Gong(龚本超), Huan-Cheng Yang(杨焕成), Kui Jin(金魁), Kai Liu(刘凯), Zhong-Yi Lu(卢仲毅)

Chin. Phys. B . 2020, 29(7): 077508 . **doi:** 10.1088/1674-1056/ab9617

Three- and two-dimensional calculations for the interface anisotropy dependence of magnetic properties of exchange-spring $Nd_2Fe_{14}B$/*α*-Fe multilayers with out-of-plane easy axes

Qian Zhao(赵倩), Xin-Xin He(何鑫鑫), Francois-Jacques Morvan(李文瀚), Guo-Ping Zhao(赵国平), Zhu-Bai Li(李柱柏)

Chin. Phys. B . 2020, 29(3): 037501 . **doi:** 10.1088/1674-1056/ab69e9

Magnetic properties of the double perovskite compound Sr_2YRuO_6

N. EL Mekkaoui, S. Idrissi, S. Mtougui, I. EL Housni, R. Khalladi, S. Ziti, H. Labrim, L. Bahmad

Chin. Phys. B . 2019, 28(9): 097503 . **doi:** 10.1088/1674-1056/ab3441

Phase diagrams and magnetic properties of the mixed spin-1 and spin-3/2 Ising ferromagnetic thin film:Monte Carlo treatment

B Boughazi, M Boughrara, M Kerouad

Chin. Phys. B . 2019, 28(2): 027501 . **doi:** 10.1088/1674-1056/28/2/027501

Mn-based permanent magnets

Jinbo Yang(杨金波), Wenyun Yang(杨文云), Zhuyin Shao(邵珠印), Dong Liang(梁栋), Hui Zhao(赵辉), Yuanhua Xia(夏元华), Yunbo Yang(杨云波)

Chin. Phys. B . 2018, 27(11): 117503 . **doi:** 10.1088/1674-1056/27/11/117503

Gd impurity effect on the magnetic and electronic properties of hexagonal Sr ferrites: A case study by DFT

Masomeh Taghipour[1], Mohammad Yousefi[2,†], Reza Fazaeli[3], and Masoud Darvishganji[4]

[1] *Department of Chemistry, Science and Research Branch, Islamic Azad University, Tehran, Iran*
[2] *Department of Chemistry, Yadegar-e-Imam Khomeni(RAH)shahr-e-Rey Branch, Islamic Azad University, Tehran, Iran*
[3] *Department of Chemistry, South Tehran Branch, Islamic Azad University, Tehran, Iran*
[4] *Department of Chemistry,Qaemshahr Branch, Islamic Azad University, Qaemshahr, Iran*

(Received 22 January 2020; revised manuscript received 31 March 2020; accepted manuscript online 28 April 2020)

The electronic and magnetic properties of strontium hexa-ferrite ($SrFe_{12}O_{19}$) are studied in pure state ($SrFe_{12}O_{19}$) and with dopant in the positions 2 and 3 of Fe atoms ($SrGdFe_{11}O_{19}$-I and $SrGdFe_{11}O_{19}$-II, respectively) by utilizing a variety of the density functional theory (DFT) approaches including the Perdew–Burke–Ernzerhof generalized gradient approximation (PBE-GGA) and GGA plus Hubbard U parameter (GGA+U). The pure $SrFe_{12}O_{19}$ is a hard magnetic half-metal with an integer magnetic moment of 64.00μ_B, while using the GGA+U functional, the magnetic intensity increases, resulting in a magnetic semiconductor with a high integer magnetic moment of 120μ_B. By doping the Gd atom in the two different positions of Fe, the magnetic moment is increased to 71.68μ_B and 68.00μ_B, respectively. The magnetic moment increases and remains an integer; hence, $SrGdFe_{11}O_{19}$-II can be very useful for application in magnetic memories. Moreover, applying the Hubbard parameter turns $SrGdFe_{11}O_{19}$-I and $SrGdFe_{11}O_{19}$-II to magnetic semiconductors with a magnetic moment of 124μ_B, and the energy gap of both doped structures at spin down is found to be less than the pure case. By studying the electronic density diagram of the atoms of the crystal, it is found that the major effect to create magnetization in the pure case is due to the Fe atom. However, in the doped case, the elements Gd and Fe have the highest moment in the crystal respectively.

Keywords: magnetic properties, density functional theory, half-metal, doping

PACS: 75.75.–c, 71.15.Mb, 61.72.–y **DOI:** 10.1088/1674-1056/ab8d9f

1. Introduction

Ferrites, a class of ceramic-like materials with magnetic properties, are useful in many types of electronic and magnetic devices. The crystal structures of ferrites are classified into 4 types, including spinel ferrites, garnet structure, ortho ferrites (perovskite), and hexagonal ferrites.[1]

Hard ferrites are important in many industrial applications such as permanent magnetic materials, electric motors,[2] microwave devices,[3] and data storage for the telecommunication,[4,5] medical,[6] and environmental uses.[7] Magneto-plumbite type hexaferrites (M type) of $AFe_{12}O_{19}$ (A = Sr, Ba, Pb) are high-performance hard magnetic materials with high Curie temperatures, high magnetism, and high magneto-crystalline anisotropy, great chemical stability, and high resistance against corrosion; these compounds are synthesized by the sol-gel method as many other hard magnetic materials.[8–13]

Structurally, the oxygen ions are positioned in the polyhedron's corners. The space group of $AFe_{12}O_{19}$ is $P63/mmc$ with five non-equivalent crystalline positions for Fe (namely 2a, 2b, $4f_1$, $4f_2$, and 12k). There are six coordination numbers of Fe for the positions 2a, $4f_2$, and 12k, five coordination numbers for 2b, and four coordination numbers for $4f_1$. The magnetic structure of the hexagonal ferrite is ferrimagnetic, in which the magnetic moments of Fe^{3+} are parallel at positions 2a, 2b, and 12k, while anti-parallel at the positions $4f_1$ and $4f_2$ along c-axis.[14]

Studies in recent years have shown that pure barium hexaferrite as one of the most famous ones among hard magnetic materials with high crystalline magnetic anisotropy along c axis can be transformed into a soft magnetic material with planar crystalline magnetic anisotropy by replacing its ions with different cations such as Fe^{3+}, Ti^{4+}, Co^{2+}, Li^{3+}, and Ce^{4+}, so that this pattern has similar results for other magneto-plumbite structures.[15] Recently, studies of the Fe^{3+} and Sr^{2+} substitution with metal and rare alkali ions have been done to improve different properties. Doping elements such as Ce, Zn, Mn, Sm, Co, Yb, and Gd has been carried out, in each of which the effects of the doped element on the magnetic behavior and electrical properties of the structure have been studied.[16–18]

Studies on garnet and perovskites and other magnetic nano-particles have also shown that doping the above elements has a significant effect on their thermal stability, crystallization, physical, magnetic, and optical properties.[19–22] The carrier doping positive effects on the magnetic properties of defective graphene have been detected.[23] Using first-principle calculations, researchers have investigated the mechanical, structural, and electronic properties and formation

†Corresponding author. E-mail: myousefi50@hotmail.com

© 2020 Chinese Physical Society and IOP Publishing Ltd

energy of 25 kinds of III–V binary monolayers in detail.[24] Different magnetic and dynamic properties studies on iron nanowire by Monte Carlo simulation and coercivity mechanisms in nanostructured permanent magnets, as well as the density functional theory (DFT) study on Dirac cones in bilayered perovskites, have been conducted in different research studies.[25–27]

In addition to investigating the different methods of experimental synthesis of these ferrites and their application in industry, there have been numerous studies on the relating computational methods using the density functional theory,[28,29] such as the calculation of exchange integrals in the strontium hexaferrite structure in order to study the antiferromagnetic exchange interactions,[30] calculation of the electronic band structure, splitting parameters investigation of the electronic properties in the doped structure, charge localization, and crystalline magnetic anisotropy in the doped structures.[31]

One of the most commonly used physical states of magnetic materials is the half-metallic state. Half-metals are a class of materials that are well-known candidates in the spintronics industry for enhancing magnetic memory, and application in tunnel magnetoresistances (TMRs) and giant magnetoresistances (GMRs).[32,33] These materials are semiconductors in one spin channel and metals in the other.[34–38] One of the problems with these materials is that the half-metallic property is often disturbed or severely decreased at the surface of the material. Thus, researchers have always been looking for a way to solve this problem, and the best way up to now, is engineering the half-metal to obtain a spin polarization state of 100% and an integer magnetic moment.[39–44]

In this work, the Gd atom with the atomic number 64 from the lanthanide family is selected for doping in strontium hexaferrite. This element has a single magnetic moment of $8\mu_B$ and is very capable for changing the physical properties of the material. After the introduction, the details and methods of calculation are presented in the second section. In the third section, after optimizing the input parameters, we study the structural properties and thermodynamic stability of the pure and doped cases. Finally, the fourth section provides the electronic and magnetic properties, followed by the conclusion in the fifth section.

2. Computational details

We performed self-consistent calculations using the WIEN2k computational code based on the density functional theory with full potential. To solve the Kohn–Sham equations governing the problem, we used the augmented plane wave method with local orbital for the valence and semi-core electrons (APW+lo). We applied the generalized gradient approximation (pbe-GGA) and GGA plus Hubbard U parameter (GGA+U) to calculate the exchange correlation potential,[39,42,43] and the space group $p63/mm3$ (194) was employed to construct the graphene flat structure, which belongs to the hexagonal space group family. The radii of proper muffin-tin spheres without overlap for Sr, Fe, O, and Gd atoms were considered 2.45 Å, 1.74 Å, 1.5 Å, and 2.21 Å respectively. We chose the cut-off radius of the wave functions in the inter-position zone regions R_kmax and G_max equal to 8 and 14 respectively. In the first Brillouin zone, we chose 500 points which were reduced to 42 points taking advantage of symmetry.

3. Investigation of the structural properties and thermodynamics stability

One of the hexagonal ferrites' family is strontium hexaferrite ($SrFe_{11}O_{19}$). In the unit cell of this structure, 64 atoms are assumed to have 24 symmetries in the crystal by applying the $p63/mm3$ (194) space group, and these 64 atomic positions are reduced to 11 atomic positions. The first position consists of two Sr atoms, the positions 2–6 consist of 24 Fe atoms, and the atomic positions 7–11 contain 38 O atoms (Fig. 1(a)).

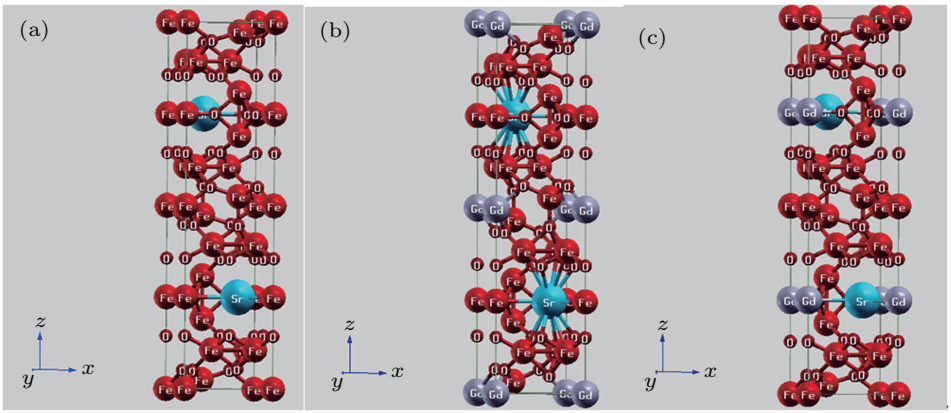


Fig. 1. (a) The $SrFe_{12}O_{19}$ structure, (b) the $SrGdFe_{11}O_{19}$-I structure, and (c) $SrGdFe_{11}O_{19}$-II structure.

In order to change the physical properties of the material, we substitute the magnetic metal Gd instead of the Fe atoms in the two positions 2 and 3, represented by $SrGdFe_{11}O_{19}$-I and $SrGdFe_{11}O_{19}$-II, respectively, as shown in Figs. 1(b) and 1(c). By introducing the Gd atoms with a larger atomic radius than Fe, the structural order of the pure crystals is slightly disrupted, and after optimizing, the bond lengths are calculated before and after substituting the impurity in all the three crystals as shown in Table 1.

Table 1. The bond lengths in the crystals $SrFe_{11}O_{19}$, $SrGdFe_{11}O_{19}$-I, and $SrGdFe_{11}O_{19}$-II.

Bond lengths	$SrFe_{12}O_{19}$	$SrGdFe_{11}O_{19}$-I	$SrGdFe_{11}O_{19}$-II
Fe–O/Å	1.8169	1.8170	1.9445
Sr–O/Å	2.9173	2.7481	2.9309
Fe–Sr/Å	3.7002	3.5483	3.7403
Gd–O/Å	–	2.2531	2.0479

As can be seen, the Gd impurity has changed the bond lengths. Changes in the crystals' structures also change their physical properties. To study the thermodynamic stability and structural properties of a crystal in computational physics, it is necessary to study the total energy of the system and its changes versus volume (E–V). For this purpose, the total energy of the crystal is calculated for different volumes and then, using a proper equation of state, namely, the Birch–Murnaghan equation, the energy as a function of volume is fitted for the pure $SrFe_{11}O_{19}$ and the doped $SrGdFe_{11}O_{19}$-II as shown in Fig. 2. Using the minimum of the E–V diagram, the equilibrium volume is calculated, then using this equilibrium volume, the appropriate lattice constants for the crystal are obtained. It is noteworthy that the existence of this minimum energy attests to the thermodynamic stability of these structures.

To study a system theoretically, one should be able to realize it at the first place. This is confirmed using some measures defining the feasibility of a system, one of which is connected to its thermodynamic stability, namely, the cohesive energy E_C (in units of eV)

$$E_C = \frac{E_{\text{total}}^{\text{SrFe}_{12}\text{O}_{19}(\text{pure,I,II})} - \left[N_{\text{Sr}}E_{\text{Sr}}^{\text{Single}} + N_{\text{Fe}}E_{\text{Fe}}^{\text{Single}} + N_{\text{O}}E_{\text{O}}^{\text{Single}} + N_{\text{Gd}}E_{\text{Gd}}^{\text{Single}}\right]}{N_{\text{Sr}} + N_{\text{Fe}} + N_{\text{O}} + N_{\text{Gd}}},$$

where $E_{\text{total}}^{\text{SrFe}_{12}\text{O}_{19}(\text{pure,I,II})}$ is the total energy of the compound, E_X^{single} and N_X (X = Sr, Fe, O, Gd) are the energy and number of the single X atoms, respectively. Here, we obtain the cohesive energy as -7.3446576 eV, -6.5765432 eV, and -6.9345642 eV for $SrFe_{12}O_{19}$, $SrGdFe_{11}O_{19}$-I, and $SrGdFe_{11}O_{19}$-II, respectively. As it is clear, all the three compounds have negative cohesive energy, confirming their thermodynamic stability.

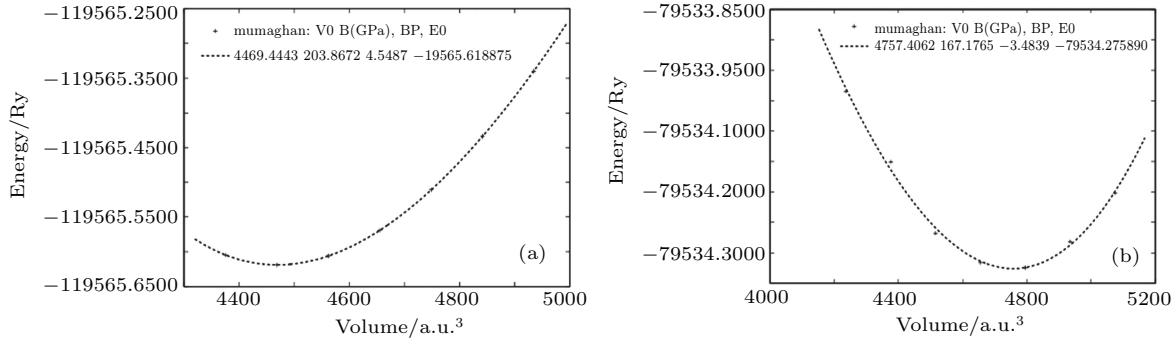


Fig. 2. The E–V diagram of (a) the pure compound $SrFe_{11}O_{19}$ and (b) the doped $SeGeFe_{11}O_{19}$-II.

4. The electronic and magnetic properties

In condensed matter physics, the most important quantities for studying the electronic and magnetic properties of the crystal are the density of states (DOS) and the band structure, which give us important information about the physical properties of the material under investigation. Figure 3 shows the total DOS diagram for the three crystals $SrFe_{12}O_{19}$, $SrGdFe_{11}O_{19}$-I, and $SrGdFe_{11}O_{19}$-II in the two spin up and down modes using the PBE-GGA functional.

In the pure $SrFe_{11}O_{19}$ crystal in spin down, the DOS diagram crosses the Fermi surface and has metallic property in this channel; but in the spin up, we see a splitting at the Fermi surface so that the compound in this channel is a semiconductor with 0.5 eV spin flip gap. This means that, overall, the crystal is a half metal. In the $SrGdFe_{11}O_{19}$-I crystal, the DOS diagram intersects the Fermi surface at both the spins up and down, representing the metallic property of this compound. However, in the $SrGdFe_{11}O$-II crystal, the material behaves like a semiconductor with a band gap of about 0.4 eV in the spin-up, which is lower than that of the pure state. At the spin down channel, on the other hand, as in the two other structures, the Fermi surface is cut by the DOS diagram, showing the metallic property, so this crystal is also a half-metal.

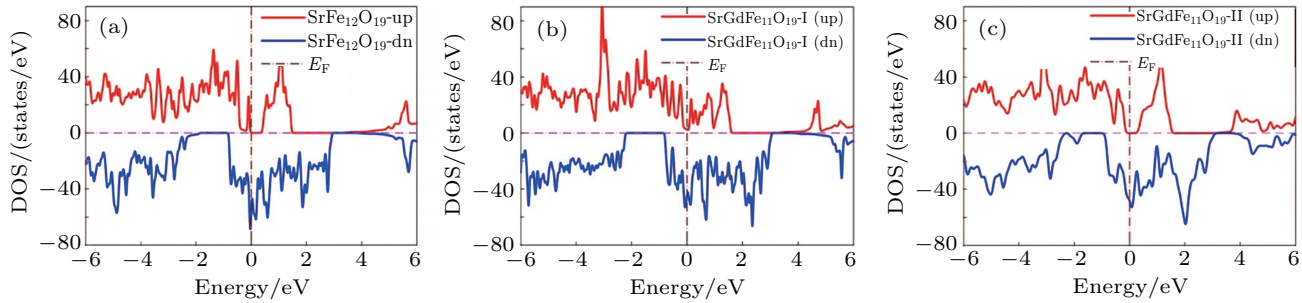


Fig. 3. Total DOS contribution of the spins up and down to (a) $SrFe_{12}O_{19}$, (b) $SrGdFe_{11}O_{19}$-I, and (c) $SrGdFe_{11}O_{19}$-II using PBE-GGA method.

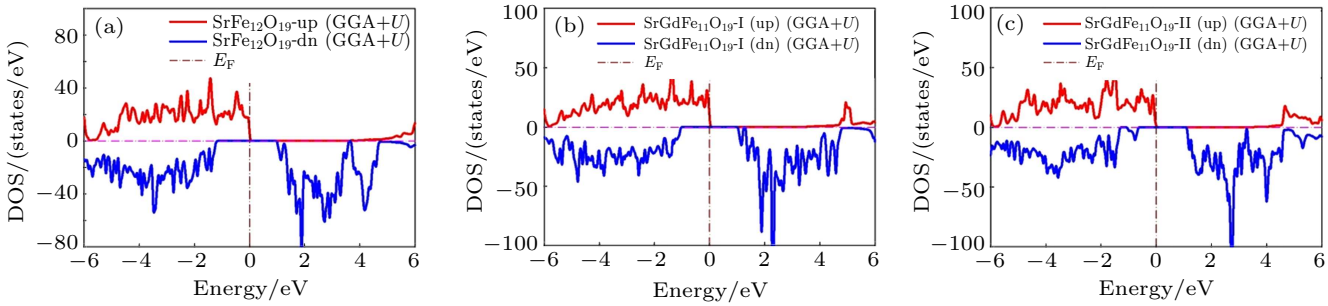


Fig. 4. The total DOS contribution of the spins up and down to (a) $SrFe_{12}O_{19}$, (b) $SrGdFe_{11}O_{19}$-I, and (c) $SrGdFe_{11}O_{19}$-II using GGA+U method.

GGA does not correctly calculate the correlation between the d and f electrons, hence, in the calculations using the computational approach, the Columbian repulsion energy (U) is calculated and used for the d and f orbitals of Fe and Gd, where $U = U_{\text{eff}}$ and $J = 0$. To study the dependence of the results on U, we apply $U = 5.3$ eV for Fe atoms and $U = 8.3$ eV for Gd, following the evaluation performed for $SrFe_{12}O_{19}$ and $SrGdFe_{11}O_{19}$-I and $SrGdFe_{11}O_{19}$-II structures. The total DOS diagram for these structures is shown in Figs. 4(a)–4(c).

Under the effect of the U parameter and the dependence of the exchange integrals on it, $SrFe_{12}O_{19}$ turns to a magnetic semiconductor and is changed significantly from the case calculated with the PBE-GGA functional. In spin up, the energy gap is increased from 0.5 eV to 3.7 eV, and in the spin down, an energy band gap of 2.27 eV is observed with a spin flip gap of about 1.0 eV. $SrGdFe_{11}O_{19}$-I and $SrGdFe_{11}O_{19}$-II are also converted to magnetic semiconductors, their electronic states change and a decrease in the spin down energy gap is observed, which are obtained as 2.12 eV and 1.80 eV, respectively.

The band structure is created by the overlap of atomic wave functions in the k space. Figure 4 shows the band structure calculated for the pure $SrFe_{12}O_{19}$ compound and in the presence of the doped Gd atom at positions 2 and 3 for the two spin states up and down with the PBE-GGA functional.

In the pure structure of $SrFe_{11}O_{19}$ and at the spin up, a spin flip gap of 0.5 eV is observed at point M, which is a direct energy gap. But in the spin down, many of energy bands cut the Fermi surface and this spin plays the major role in electron transport. In the presence of the impurity Gd at position 2 in both spins up and down, the energy bands cut the Fermi energy, resulting a metallic nature; due to high density of the bands in spin down, again, the electron transport is expected in this spin channel. In the presence of the impurity Gd at position 3, i.e., in $SrGdFe_{11}O_{19}$-II at spin up, an indirect energy band gap of about 4 eV is observed in the band structure, which is less than that of the pure case. In spin down, the density of the bands is also extremely high which is clearly proportional to the DOS diagram at the Fermi level.

The most important aspect of ferrites is their high magnetic properties, making them highly useful in the electronics industry. The magnetic property of a material depends on the magnitude of its magnetic moments of the atoms forming that material and the interaction of the moments. Fully filled orbitals have no contribution to the magnetic moment, while the filling orbitals have a major role. Most of the magnetic moment relates to free atoms and ions, which causes permanent magnetic moment so the material becomes ferrimagnetic. The Gd atom from the lanthanide elements group has the electron arrangement of $[Xe]4f^7 5d^1 6s^2$, which in isolation has a high magnetic moment of about $8\mu_B$ and we expect to find more interesting properties by injecting this element into $SrFe_{12}O_{19}$. By comparing the total DOS diagram in the spins up and down, one can guess the magnetic or non-magnetic state of the crystal, and the more asymmetric both the up and down diagrams are, the stronger the magnetic properties of the material are. According to the DOS diagram of the all crystals in Figs. 3 and 4, and the band structure in Fig. 5, it is clear that the spins up and down diagrams in all three structures are completely asymmetric with respect to the horizontal line, so that all the three crystals have magnetic behavior.

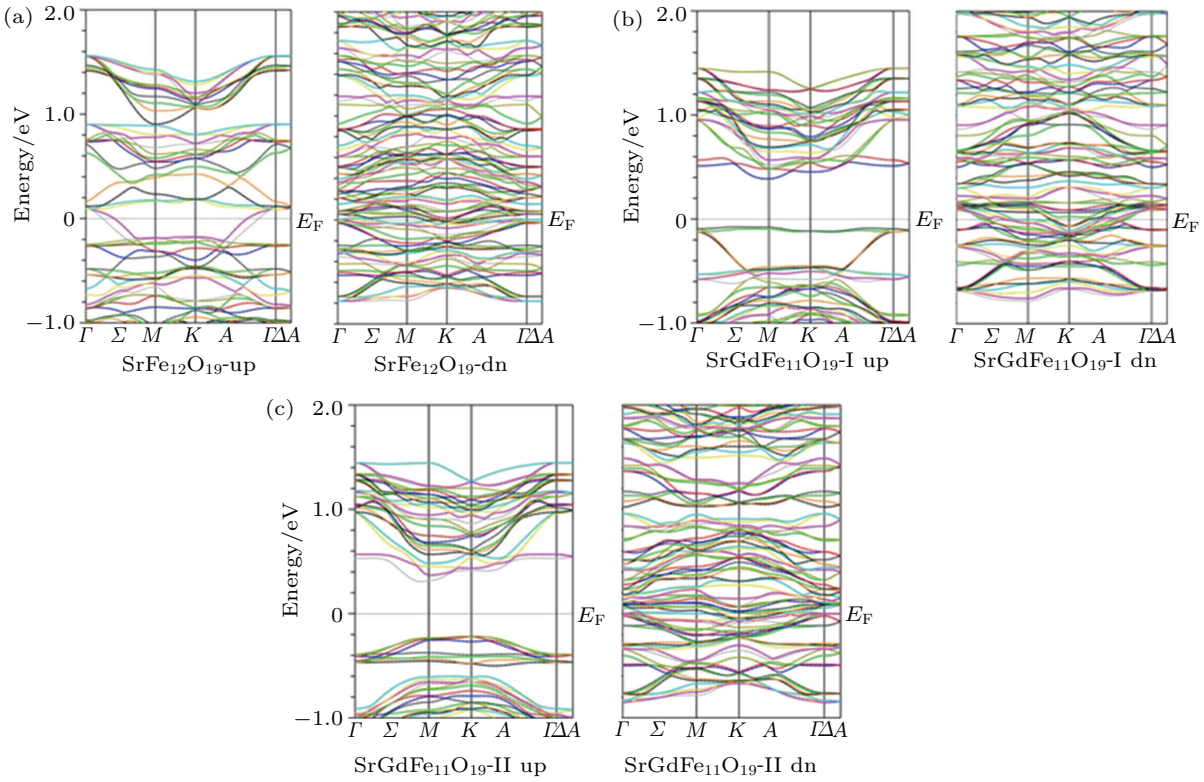


Fig. 5. Band structure for (a) pure $SrFe_{12}O_{19}$, (b) $SrGdFe_{11}O_{19}$-I, and (c) $SrGdFe_{11}O_{19}$-II.

One of the problems with magnetic materials, especially the Heuslers, is that their half-metallic properties are often disrupted or severely reduced.[45–47] One way to solve this problem, and the best one up to now, is to look for a polarization state of 100%, or in other words, the magnetic moment of the whole crystal being an integer. In Table 2, we summarize the total and partial magnetic moments of the constituent atoms for all the three structures mentioned above using the PBE-GGA functional. In the pure crystal $SrFe_{12}O_{19}$, the total magnetic moment is $64\mu_B$, which is a large integer number. Therefore, strontium hexaferrite is a hard magnetic material with a high magnetization intensity. Observing the partial magnetic moment of the atoms, it is expected that the Fe atom has the greatest influence on the crystal magnetization, and this is due to the half-filled d orbitals of this element, while the contribution of Sr and O is nearly negligible. The atoms at the positions 2 and 6 have less magnetic moments than the three Fe atoms. We therefore perform the substitution action of the Gd atom once for the Fe atoms in position 2 and once for position 3. In the $SrGdFe_{11}O_{19}$-I crystal, according to Table 2, we obtain a total magnetic moment of $71.68\mu_B$ which is higher than the pure state, i.e., the magnetic moment in this crystal is increased relative to the pure state. The results indicate that the Gd atom with $6.86\mu_B$ has the major effect on intensifying the magnetization of the entire crystal. However, the moment of Gd atom is less than that of its isolated state, which is because of hybridization between the orbitals of adjacent atoms when Gd is placed in the crystal. The remarkable point about this structure is that the total magnetic moment is not an integer, which can affect the magnetic stability of this material and may decrease its intensity over time.

By substituting the Gd atom in the atomic position 3 with two symmetric Fe atoms, the structure of $SrGdFe_{11}O_{19}$-II is formed. As can be seen in Table 2, the total magnetic moment obtained for this structure is $68\mu_B$ which is higher than the pure state but lower than the $SrGdFe_{11}O_{19}$-I. The remarkable point about this structure is that the total magnetic moment is an integer which can be very useful, because the doped crystal is a hard magnetic material and its magnetic intensity has also increased. We should note that, the magnetic properties of these structures change drastically by applying the Hubbard parameter. In $SrFe_{12}O_{19}$, the magnetic moment is increased steadily from $64.00\mu_B$ to $120.0\mu_B$, which is in good agreement with a previous report.[48] However, similar to the pure state from a magnetic point of view, by introducing the Gd atom, the magnetic intensity increases to $124.0\mu_B$ for both $SrGdFe_{11}O_{19}$-I and $SrGdFe_{11}O_{19}$-II compounds.

For a closer look at the electronic and magnetic properties of these structures, the electronic density of states graph of the atoms forming these crystals, which specifies the bond type and the contribution of the atoms to the total DOS diagram, can be very beneficial. Due to the more interesting and practical magnetic properties of $SrGdFe_{11}O_{19}$-II than the other structure, the DOS diagrams of the atoms of this crystal are shown in Fig. 6 for the two spins up and down using the PBE-GGA functional.

Table 2. Atomic magnetic moments (AMMs) of the atoms, together with the total magnetic moment (TMM) of $SrFe_{12}O_{19}$, $SrGdFe_{11}O_{19}$-I, and $SrGdFe_{11}O_{19}$-II.

	$SrFe_{11}O_{19}/\mu_B$		$SrGdFe_{11}O_{19}$-I/μ_B		$SrGdFe_{11}O_{19}$-II/μ_B	
TMM	64.00		71.68		68.00	
AMM-atom 1	Sr	0.00250	Sr	0.00677	Sr	0.01312
AMM-atom 2	Fe	1.33087	Gd	6.86616	Fe	1.26978
AMM-atom 3	Fe	3.65864	Fe	3.19686	Gd	6.82858
AMM-atom 4	Fe	3.37430	Fe	3.27279	Fe	3.29875
AMM-atom 5	Fe	3.57487	Fe	3.10673	Fe	3.44749
AMM-atom 6	Fe	1.35474	Fe	1.33457	Fe	1.32777
AMM-atom 7	O	0.05646	O	0.02623	O	0.01662
AMM-atom 8	O	0.11468	O	0.12319	O	0.10521
AMM-atom 9	O	0.32360	O	0.19861	O	0.16119
AMM-atom 10	O	0.09990	O	0.12767	O	0.09267
AMM-atom 11	O	0.11669	O	0.10424	O	0.09867

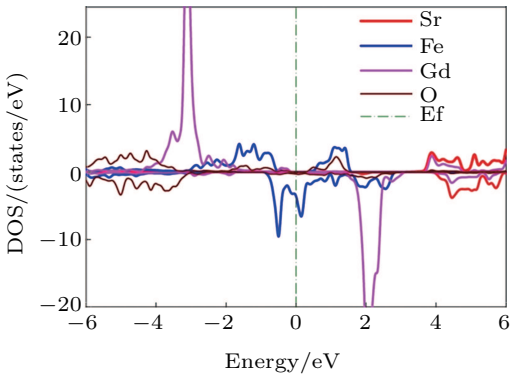


Fig. 6. PDOS of the $SrGdFe_{11}O_{19}$-II structure.

As in the figure, the major effect of the Gd atom is in the valence region with the energy of −2.7 eV to −4.2 eV. Around the Fermi surface, the iron atom contribution is higher than the other elements. Also, due to the strong differences in the peaks of the density of states and the non-complete overlap, the bond type in this material is ionic. Unlike the spin up state, the maximum impact of the Gd atom in the spin down channel is in the conduction region with the energy range of 1.5 eV to 2.7 eV; and this has intensified the magnetic state of the crystal. However, at the Fermi level, the dominant state still belongs to the Fe atoms.

The more asymmetric diagram of an atom at the spins up and down corresponds to more effects on the magnetization of that material. As can be seen, the most asymmetric cases are Gd and Fe, so they have the most influence on the total crystal magnetization. The two DOS diagrams of the two atoms Sr and O are more symmetrical, and as observed in the magnetic moment of these atoms, their effect on the magnetization of the crystal is much less.

5. Conclusion

The structural properties, thermodynamic stability, and electronic and magnetic properties of $SrFe_{12}O_{19}$ hexa-ferrite are first studied at pure state using the PBE-GGA and GGA+U functionals. The E–V diagram shows that this structure is thermodynamically quite stable. The examination of the DOS and the band structure diagrams with PBE-GGA reveals that the crystal is a magnetic half metal with a total magnetic moment of $64\mu_B$. The partial magnetic moments of the crystal atoms show that the Fe atoms have the most influence on the crystal magnetization. The Fe atoms demonstrate different magnetization and are divided into two groups from the point of view of magnetization intensity, which we have labeled as the positions 2 and 3, with the position 3 having a much higher magnetization. In the next step in the two separate structures, instead of Fe atoms, we have replaced Gd from the lanthanide family into the positions 2 and 3. In the $SrGdFe_{11}O_{19}$-I structure where the substituted atom is in position 2, the magnetic moment is significantly increased but it is non-integer. From the electronic point of view, the material becomes a magnetic metal. However, in the $SrGdFe_{11}$O-II crystal, where the Gd atom is in the position 3, an integer magnetic moment of $68\mu_B$ is obtained which is larger than the pure state. Hence, this structure can be very applicable in the magnetic memory industry, since, beside magnetic stability, it has a higher magnetic moment than the pure state. By investigating the electronic structure, $SrGdFe_{11}O_{19}$-II is found to be a half metal, with conducting and semiconducting behavior at spins down and up, respectively, albeit with a lower energy band gap compared to the pure case. By obtaining the magnetic moment as well as the DOS diagram of the atoms constituting the structure of $SrGdFe_{11}O_{19}$-II, it is found that the major effect on the magnetization intensity is related to the Gd and Fe atoms respectively. Utilizing the Hubbard parameter in these calculations, all the three compounds become magnetic semiconductors. However, the spin down gap is reduced by doping the Gd atom. The magnetic moment sharply increases and is obtained as $120\mu_B$ and $124\mu_B$ for the pure state and the other two structures respectively. Thus, the increase of the magnetic moment with doping the Gd atom is confirmed using both PBE-GGA and GGA+U functionals.

References

[1] Goldman A 1990 *Modern Ferrite Technology* (New York: Van Nostrand Reinhold) p. 69
[2] Shekhawat D, Singh A K and Roy P 2019 *J. Mol. Struct.* **1179** 787
[3] Dong S, Lin C and Meng X 2019 *J. Alloys Compd.* **783** 779
[4] Bhattacharya P, Dhibar S, Hatui G, Mandal A, Das T and Das C K 2014 *Rsc Adv.* **4** 17039
[5] Feng G, Zhou W, Deng H, Yang M, Qing Y, Luo F, Zhu D, Huang Z, Zhou Y and Wang C 2019 *J. Mater. Sci.: Mater. Electron.* **30** 12382
[6] Ren A, Qing M, Zhao N, Wang M, Gao G, Yang X, Zhang Z, Hu F, Rehman M U and Abbasi Q H 2018 *IEEE Access* **6** 29551
[7] Xie T, Hu J, Yang J, Liu C, Xu L, Wang J, Peng Y, Liu S, Yin X and Lu Y 2019 *Nanomaterials* **9** 735
[8] Abdollahi F, Yousefi M, Hekmati M, Khajehnezhad A, Afghahi S and Salman S 2019 *J. Nanostruct.* **9** 579
[9] Ghezelbash S, Yousefi M, Hossainisadr M and Baghshahi S 2018 *IEEE Trans. Magn.* **54** 1
[10] Liu C, Kan X, Liu X, Feng S, Hu J, Wang W, Rehman K M U and Shezad M 2020 *Ceram. Int.* **46** 171
[11] Liu D, Gao S, Jin R, Wang F, Chu X, Gao T and Wang Y 2019 *Chin. Phys. B* **28** 057503
[12] Mesdaghi S, Yousefi M and Mahdavian A 2019 *Mater. Chem. Phys.* **236** 121786
[13] Veisi S S, Yousefi M, Amini M, Shakeri A and Bagherzadeh M 2019 *J. Alloys Compd.* **773** 1187
[14] Pullar R C 2012 *Prog. Mater. Sci.* **57** 1191
[15] Xia A, Du D, Li P and Sun Y 2011 *J. Mater. Sci.: Mater. Electron.* **22** 223
[16] Niazi N, Farooq O, Tuz Zahra F and Anis-ur-Rehman M 2018 *Trans. Tech. Publ.*, September 18–19, 2018 Switzerland, p. 195
[17] Yasmin N, Abdulsatar S, Hashim M, Zahid M, Gillani S F, Kalsoom A, Ashiq M N, Inam I, Safdar M and Mirza M 2019 *J. Magn. Magn. Mater.* **473** 464
[18] Yasmin N, Iqbal M Z, Zahid M, Gillani S F, Ashiq M N, Inam I, Abdulsatar S, Safdar M and Mirza M 2019 *Ceram. Int.* **45** 462
[19] Chen Z, Zhu Q K, Zhang S L, Zhang K W and Jiang Y 2019 *Chin. Phys. B* **28** 087502
[20] Feng Y Q, Jin K J, Ge C, He X, Gu L, Yang Z Z, Guo H Z, Wan Q, He M and Lu H B 2016 *Chin. Phys. Lett.* **33** 076801
[21] Kuila M, Hussian Z and Reddy V R 2019 *Thin Solid Films* **691** 137593
[22] Guo M C, Liu W F, Wu P, Zhang H, Xu X L, Wang S Y and Rao G H 2015 *Chin. Phys. Lett.* **32** 066101
[23] Lei S L, Li B, Huang J, Li Q X and Yang J L 2013 *Chin. Phys. Lett.* **30** 077502
[24] Liu X F, Luo Z J, Zhou X, Wei J M, Wang Y, Guo X, Lv B and Ding Z 2019 *Chin. Phys. B* **28** 086105
[25] Chen X, Liu L and Shen D 2019 *Chin. Phys. B* **28** 077106
[26] Ye Q Y, Wang W J, Deng C C, Chen S Y, Zhang X Y, Wang Y J, Huang Q Y and Huang Z G 2018 *Acta Phys. Sin.* **68** 107502
[27] Zhao G, Zhao L, Shen L, Zou J and Qiu L 2019 *Chin. Phys. B* **28** 077505
[28] Feng M, Shao B, Lu Y and Zuo X 2014 *J. Appl. Phys.* **115** 17D908
[29] Luo Q, Yang H, Guo P and Zhao J F 2019 *Acta Phys. Sin.* **68** 169101
[30] Park J, Hong Y K, Lee W, Choi B C and Choi C J 2015 *IEEE Magn. Lett.* **7** 1
[31] Chlan V, Kouřil K, Uličná K, Štěpánková H, Töpfer J and Seifert D 2015 *Phys. Rev. B* **92** 125125
[32] Ono K, Okabayashi J, Mizuguchi M, Oshima M, Fujimori A and Akinaga H 2002 *J. Applied Physics* **91** 8088
[33] Wang X, Khachai H, Khenata R, Yuan H, Wang L, Wang W, Bouhemadou A, Hao L, Dai X and Guo R 2017 *Sci. Reports* **7** 1
[34] Akinaga H, Manago T and Shirai M 2000 *Jpn. J. Appl. Phys.* **39** L1118
[35] Alijani V, Winterlik J, Fecher G H, Naghavi S S and Felser C 2011 *Phys. Rev. B* **83** 184428
[36] De Groot R, Mueller F, Van Engen P and Buschow K 1983 *Phys. Rev. Lett.* **50** 2024
[37] Galanakis I, Ostanin S, Alouani M, Dreyssé H and Wills J 2000 *Phys. Rev. B* **61** 4093
[38] Mizuguchi M, Akinaga H, Manago T, Ono K, Oshima M, Shirai M, Yuri M, Lin H, Hsieh H and Chen C 2002 *J. Appl. Phys.* **91** 7917
[39] Balke B, Fecher G H, Kandpal H C, Felser C, Kobayashi K, Ikenaga E, Kim J J and Ueda S 2006 *Phys. Rev. B* **74** 104405
[40] Boochani A, Nowrozi B, Khodadadi J, Solaymani S and Jalali-Asadabadi S 2017 *J. Phys. Chem. C* **121** 3978
[41] Candan A, Uğur G, Charifi Z, Baaziz H and Ellialtıoğlu M 2013 *J. Alloys Compounds* **560** 215
[42] Gabor M, Petrisor Jr T, Tiusan C, Hehn M and Petrisor T 2011 *Phys. Rev. B* **84** 134413
[43] Karthik S, Rajanikanth A, Takahashi Y, Ohkubo T and Hono K 2007 *Acta Materialia* **55** 3867
[44] Rai D, Shankar A, Ghimire M and Thapa R 2012 *Physica B* **407** 3689
[45] Blaha P, Schwarz K, Sorantin P and Trichey S 1990 *Comput. Phys. Commun.* **59** 399
[46] Schwarz K 2003 *J. Solid State Chem.* **176** 319
[47] Perdew J P, Chevary J A, Vosko S H, Jackson K A, Pederson M R, Singh D J and Fiolhais C 1992 *Phys. Rev. B* **46** 6671
[48] Lyogenkaya A, Grechnev G, Kotlyar O, Panfilov A and Gnezdilov V 2016 *Ukr. J. Phys.* **61** 523